analytical chemistry

ARTICLE

pubs.acs.org/ac

One-Step Homogeneous Protein Detection Based on Aptamer Probe and Fluorescence Cross-Correlation Spectroscopy

Xiaoming Zhou, Yonghong Tang, and Da Xing*

MOE Key Laboratory of Laser Life Science & Institute of Laser Life Science, College of Biophotonics, South China Normal University, Guangzhou 510631, China

Supporting Information

ABSTRACT: A new protein assay based on fluorescence cross-correlation spectroscopy (FCCS) and aptamer probe is developed. In this assay, two spectrally distinct fluorophores labeled aptamer probes are used to recognize and detect thrombin through a sandwich reaction. The sandwich complexes are diffused through a confocal detection volume. The cross-correlation signals can be observed only at the presence of the aptamer probes-protein sandwich complexes. Thrombin is selected as a target to validate the assay. The whole detection process can be completed within an hour with low-nanomolar sensitivity and high specificity. The novel aptamer-based FCCS detection offers a simple, rapid and sensitive method for protein analysis in a homogeneous format.

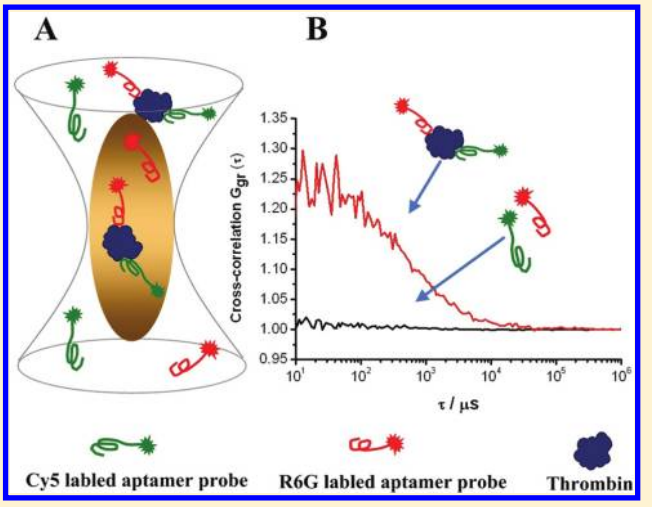

Rapid and sensitive detection of the proteins is of important for many applications, such as medical diagnostics, pharmaceutical development, and proteomics research. The most commonly used method for protein detection is enzyme-linked immunosorbent assay (ELISA).[1,2] However, ELISA requires multiple steps and long incubation periods (≥1 h per step) and can only achieve a semiquantitative result. Fluorescence techniques are rapidly becoming a leading tool in life sciences because of its versatility, potential for multiplexing, ease of use, and remarkable sensitivity. The detection of proteins with fluorescence techniques based on antibody sandwich-type immunoassay is continually being studied.[3−8]

Now aptamers are starting to show their versatility in developing a variety of biosensors. Systematic evolution of ligands by exponential enrichment (SELEX) is the original method for producing aptamers in vitro.[9,10] The adaptation of aptamers to function as biosensors would potentiates numerous diagnostic applications.[11−17] Compared to antibody, aptamers are small nucleic acids that can be selected under very general conditions and produced by chemical synthesis, without the constraints imposed by having to be selected or produced in lab animals.[18] Several aptamer-based fluorescence methods for protein detection have been developed.[11] They can be categorized into heterogeneous and homogeneous formats. Heterogeneous assay involves a separation step prior to signal measurement, thus suffers from disadvantages associated with laborious steps, and health-related risks. Homogeneous assay is a direct detection method that can be carried out without any need of separation process.

To the authors' knowledge, currently available homogeneous aptasensors are mainly based on fluorescence polarization and fluorescence resonance energy transfer (FRET) techniques.[19−23] However, both approaches are impractical to directly analyze proteins in their native environments due to the interference of background signals. A novel and more practical homogeneous system is still needed for improving modern biomedical research.

Dual-color fluorescence cross-correlation spectroscopy (FCCS), realized experimentally first by Schwille et al.,[24,25] is an extended version of fluorescence cross spectroscopy (FCS).[26−29] In the FCCS system, two spectrally distinct fluorophores in the same target volume are independently excited. Simultaneous fluctuations of the fluorescence signals indicate the presence of tight chemical or physical linkages between the fluorophores. In FCCS, analyte molecules diffuse in and out of the femtoliter probe volume yield interesting information. The system allows for probing of extremely low fluorophore concentrations with a

Received: November 1, 2010
Accepted: February 28, 2011
Published: March 17, 2011

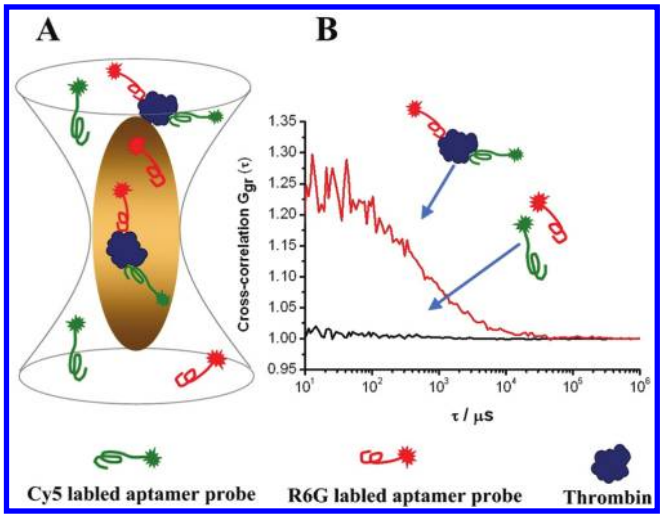

Figure 1. Strategy for one-step homogeneous protein detection based on aptamer probe and single-molecule fluorescence spectroscopy. (A) aptamer probes labeled with green and red fluorophores along or interacted with protein are diffused through a confocal detection volume. (B) The resulting fluctuations of the fluorescence of both fluorophores are detected and are cross-correlated. The amplitude of the cross correlation function $G_{gr}(t)$ is proportional to the fraction of particles carrying both fluorophores.

separation-free format.[6−8,30−36] This tool is considered as a "true" single-molecule measurement.[37]

In this work, we have developed a new protein assay based on FCCS and aptamer probe. In this assay, two spectrally distinct dyes labeled aptamer probes were used to recognize and detect thrombin through a sandwich reaction. The sandwich complexes are diffused through a confocal detection volume (Figure 1A). The cross-correlation signals can be observed only at the presence of the aptamer probes-protein sandwich complexes (Figure 1B). The presence of the double-labeled particles in the mixture is detected with nanomolar sensitivity by FCCS. Thrombin is selected as the target to validate the assay. Thrombin is a protein that plays important roles in the coagulation cascade, thrombosis, and hemostasis.[38] Changes in thrombin concentration levels in blood is known to be associated with some diseases.[39]

MATERIALS AND METHODS

Chemicals and Materials. Pure human α-thrombin was supplied by Haematologic Technologies Inc. (ESSEX Junction, VT). AFP and lgE were purchased from Roche diagnostics Corporation. Bovine serum albumin was produced by GuangZhou ZhanChen biologic-tech Co., Ltd., China. Phosphate buffered saline (phosphate salt, 0.01 M; NaCl, 0.138 M; KCl, 0.0027 M; $MgCl_2$, 0.002 M; pH 7.4) was used throughout the experiments. Eight wells Lab-Tek chambered coverglass was purchased from Nunc (Thermo Fisher Scientific).

Labeling of Aptamer Probes. The two aptamers used in this study that were purified by HPLC and have the following sequences: Apt15, RG-tttttggttggtgtggttgg, Apt29, Cy5-tagtccgtggtagggcaggttggggtgact. Apt15 is a relatively short 15-base DNA aptamer, which binds exosite I of thrombin (fibrinogen binding sites).[40] A 29-base DNA aptamer, referred to as Apt 29, which binds to exosite II of thrombin (a heparin-binding aptamer).[41] We labeled RG and Cy5 dyes into the Apt15 and Apt29, respectively. RG and Cy5 labels were chosen because of their distinctive excitation spectra and their well-separated emission profiles, as well as because of their low energy transfer with the DNA target.[30,42]

Sample Preparation. Breifly, two dye-labeled aptamer probes were heated to 95 °C for 2 min, and then cooled to 4 °C to ensure a single-stranded structure. The two aptamer probes were then incubated with thrombin or thrombin spiked serum samples in bind buffer (phosphate salt, 0.01 M; NaCl, 0.138 M; KCl, 0.0027 M; $MgCl_2$, 0.002 M; pH 7.4). After the binding of thrombin (30 min), the mixtures were used for FCCS experiments.

FCCS Measurements. FCCS measurements were carried out with a ConfoCor2 system (ConfoCor2, Carl Zeiss, Jena, Germany), which allows simultaneous excitation at 488 and 633 nm (Argon and HeNe laser, respectively) and the detection of the emission in the green (band-pass filter 505 ± 550 nm) and red (long-pass filter 650 nm) wavelength range by avalanche photodiodes. The sample was contained in a 8 wells Lab-Tek chambered coverglass with a cover glass on top, and was then placed on the stage of an inverted microscope (Axiovert 200M; Zeiss). The confocal pinhole diameter was adjusted to 70 μm for 488 line and 90 μm for 633 line. The excitation intensities were adjusted to 25 μW for HeNe2 laser line and 100 μW for Argon laser line.

The excitation light was reflected by a dichroic mirror and focused on the focal plane within the sample by an objective (C-Apochromat ×60/1.2). The emitted fluorescent light was collected by a high numerical aperture objective and passed through the dichroic mirror, which reflected the excitation light toward the objective and transmitted the fluorescent light. The residual laser excitation light and Raman scattered light were removed by additional band-pass filters. Each sample was measured three times (120 s each measurement), and the results were averaged. The data from the samples were averaged and the auto- and cross-correlation functions were obtained.

Data Analysis. In dual-color FCCS, the aptamer probes labeled by two different fluorescent dyes and bind with the target protein can be excited simultaneously by two different laser beams and the fluorescence signals from the dyes can be detected in two separate channels. The cross-correlation function between the fluorescence intensities of green (g) and red (r) dyes, $G_{gr}(\tau)$, can be determined. The cross-correlation function can be described as

$$G_{gr}(\tau) = 1 + \frac{1}{N_\times}\left\{\left(1 + \frac{\tau}{\tau_{diff,gr}}\right)\sqrt{1 + \frac{\tau}{S^2\tau_{diff,gr}}}\right\}^{-1} \quad (1)$$

where $\tau_{diff,gr}$ is the diffusion time of the thrombin bind with both green and red dyes labeled probes and $N_\times$ is the inverse amplitude of the cross-correlation function

$$N_\times = \frac{1}{G_{gr}(0) - 1} \quad (2)$$

Assuming that there is no cross-talk between the two detection channels, the number of doubly labeled molecules in the detection volume, N_{gr}, can be determined by

$$N_{gr} = \frac{N_{ac,g} \times N_{ac,r}}{N_\times} \quad (3)$$

where $N_{ac,g}$ and $N_{ac,r}$ are the numbers of the singly labeled

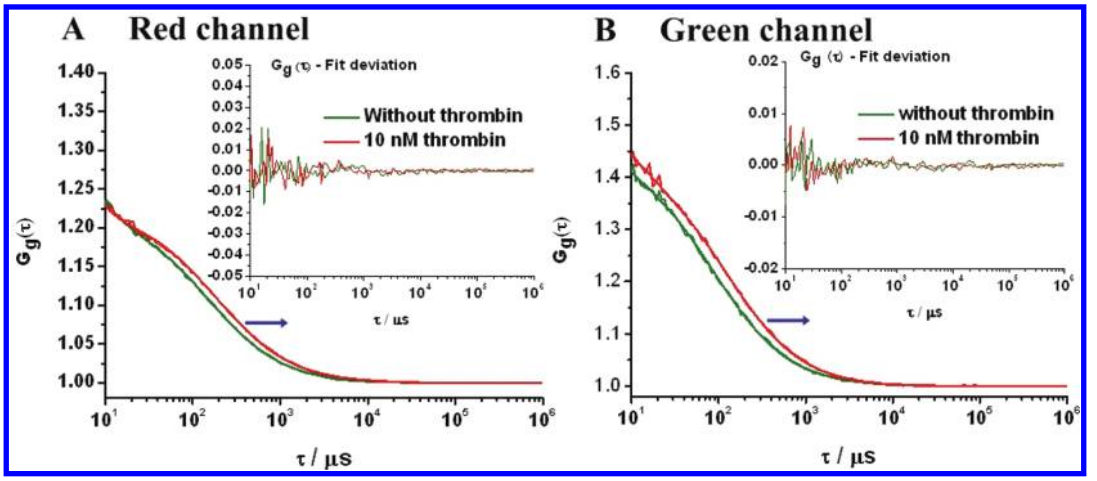

Figure 2. Normalized fluorescence autocorrelation function. The arrow indicates the shift of fluorescence autocorrelation function with (red line) and without (green line) of 10 nM thrombin. (A) Apt29 and thrombin. (B) Apt15 and thrombin. (Insets) shows the residuals of the fit.

aptamer in the detection volume obtained from the autocorrelation functions according to eq 4 in the green and red detection channels, respectively.

$$G(\tau) = 1 + \frac{1}{N}\left\{\left(1 + \frac{\tau}{\tau_{diff}}\right)\sqrt{1 + \frac{\tau}{S^2\tau_{diff}}}\right\}^{-1} \quad (4)$$

The correlation data set of obtained was fitted to the autocorrelation and cross-correlation function according to eq 5, taking into account the triplet state build-up.

$$G(\tau) = 1 + \frac{1}{N_{eff}}\left\{\frac{1 - F_{trip} + F_{trip}\times\exp(-\tau/\tau_{trip})}{1 - F_{trip}}\left(1 + \frac{\tau}{\tau_{diff}}\right)\sqrt{1 + \frac{\tau}{S^2\tau_{diff}}}\right\}^{-1} \quad (5)$$

where τ_{trip} and F_{trip} are the decay time of the triplet state and fractional population, respectively. N_{eff} is the corrected particles number.

Quantitative cross-talk ($G_\kappa(0)$) assessment can be achieved by following equation:[25]

$$G_\kappa(0) = \kappa_{gr}(F_g/F_r) \times G_g(0) \quad (6)$$

where $G_\kappa(0)$ is the green autocorrelation curve at $t = 0$, the bleed-through ratio $\kappa_{gr} = F_r^{calibr}/F_g^{calibr}$, F_r^{calibr} is the count rate in red channel and F_g^{calibr} is the count rate in green channel measured from a sample with only green-labeled particles. F_g and F_r are the count rate in green and red channels in the actual measurements.

RESULTS

It is reported in literature that the quantum yield of a dye can be influenced by the sequence of the attached oligonucleotide.[43,44] Quantum yield of RG is reduced via interaction with guanine.[43] Addition of a dT linker can result in a significantly reduced fluorescence quenching of the dye by guanine.[44] In our preliminary study, we have compared two RG labeled aptamer probes (RG-ggttggtgtggttgg and RG-tttttggttggtgtggttgg) for their fluorescence characteristics. Figure S1 shows the fluorescence count rates between the probes (5 nM) with and without a 5 dT spacer. It is found that a greater than 30% fluorescence quenching for RG labeled Apt 15 without a 5 dT linker. We thus added a linker sequence ($d(T)_5$) to the 5′ of Apt15 to minimize the potential reduction in RG quantum yield.

Due to a small confocal detection volume ($V_{eff} \approx 0.5$ fL) in the current FCCS detection, a strong binding interaction is required to obtain detectable bound species. Single-color FCS measurements are first performed to confirm the binding between the aptamer and thrombin. FCS derives information from temporal fluctuations in fluorescence signals caused by the diffusion of fluorescent particles through a confocal detection volume. Binding of a mass target to a fluorophore labeled probe slows down the diffusion of the probe, thus resulting in a right shift of the autocorrelation function $G_{(t)}$ toward a longer autocorrelation time. To distinguish the two components in FCS analysis, their diffusion times must differ by a factor of at least 1.6. This corresponds to a molecular weight ratio of 4.[45] In this study the molecular weight of labeled Apt15 and Apt29 is 6.2 and 9.3 kDa. Molecular weight of human thrombin is 35 kDa. The molecular weight ratio of the Apt15-thrombin to Apt15 is 6.6, and Apt29-thrombin complex to Apt29 is 4.7, respectively. Both values are sufficiently above the mentioned criterion of 4. In our measurements, the diffusion times of Apt15 and Apt29 in the bind buffer were 80 ± 6 and 116 ± 5 μs, respectively. After of the incubation with thrombin, the corresponding diffusion times increased to 131 ± 9 and 175 ± 15 μs. Figure 2 shows that the normalized autocorrelation function of both Apt15 and Apt29 shifted to the right after the addition of 10 nM thrombin. This indicates the binding of thrombin and the corresponding aptamer occurs. We noted that this experiment using FCS should not be construed as an effective protein assay; the sensitivity of FCS is restricted by the limited diffusion difference. In more complex systems, diffusion coefficient measurements lack the specificity needed to assign an observable mobility change to its corresponding binding process.

In contrast, the cross-correlations only occur when two dye-labeled aptamer probes are either bound to each other or bound to thrombin. In following experiments, two aptamer probes were incubated with thrombin in the bind buffer. FCCS measurements were performed to address these characteristics. The cross-correlations are functions of the diffusion time and the concentration of the complexes (Apt15-thrombin-Apt29). The intercept of the curve is dependent on the concentration of the double labeled complexes. The cross-correlation signals as well as both

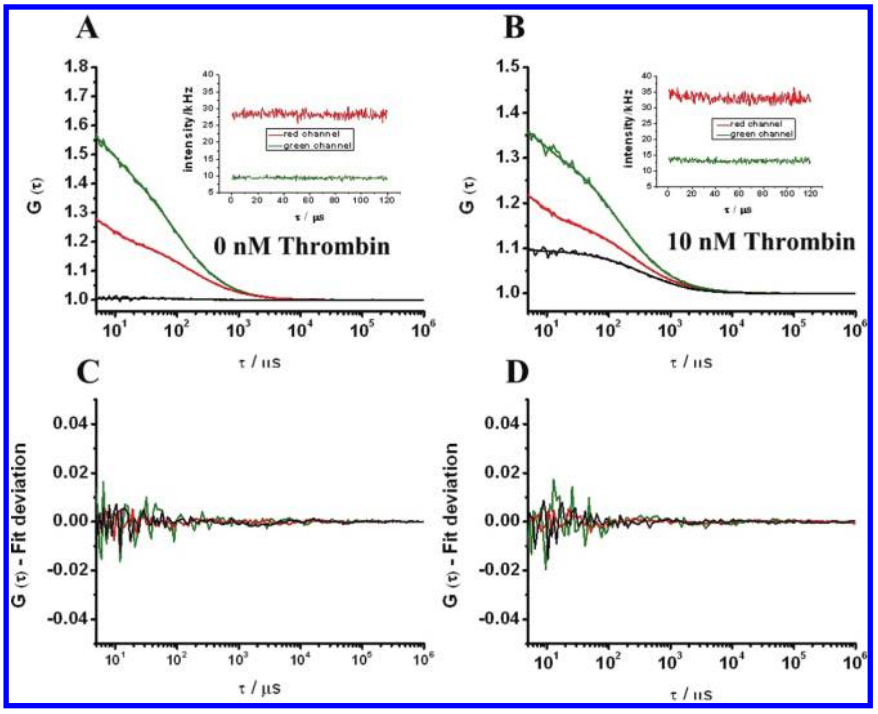

Figure 3. Typical auto- and cross-correlation curves of detection of (A) 0 thrombin, (B) 10 nM thrombin. Inset shows the fluorescence intensities in red and green channels during FCCS measurement. Red line indicates the autocorrelation curves from Cy5 labeled Apt29; green line indicates the autocorrelation curves from RG labeled Apt15; black line indicates the cross-correlation curves. (C) and (D) show the residuals of the fit.

autocorrelation signals are displayed for comparison (Figure 3A and B). As shown in Figure 3A, cross-correlation amplitude close to 1 was detected when the two dye-labeled aptamer probes physically mixed in the binding buffer in absence of thrombin. In comparison, high-levels of cross-correlation was observed for detecting 10 nM thrombin (Figure 3B).

In current study, two spectrally well-distinct fluorophores (Cy5 and RG) are used to label the aptamer probes. Because of the FCCS is an assay with accuracy at single molecule level, artifact risks may arise from cross-talk even in the presence of tiny spectral bleed-through. For cross-talk assessment, only a few percent of bleed-through from the green into the red channel needs to be considered, while there is minimal bleed-through from the red into the green channel. Quantitative cross-talk ($G_\kappa(0)$) assessment can be achieved with eq 6. We have performed some calibration measurements and a κ_{gr} of about ≈ 0.03 was established. According to the equation, the $G_\kappa(0)/G_g(0)$ obtained from our measurements is $\sim$0.015. This is significantly lower than the observed relative cross-correlation (see in table 1). Owing to this very low value of $G_\kappa(0)$, the cross-correlation functions were not corrected for cross-talk.

The count rate of RG labeled Apt15 and Cy5 labeled Apt29 at 0 nM thrombin were 9.4 $\pm$ 0.3 kHz and 28.2 $\pm$ 0.8 kHz, respectively. In the presence of 10 nM thrombin, the intensities were 13.1 $\pm$ 0.5 and 33 $\pm$ 1.1 kHz, respectively. The data indicated that the addition of thrombin resulted in minimal change in fluorescence intensities of both dyes. Energy transfer effect was negligible because there is no significant difference between them.

The fits and residuals for the correlation data are shown in Figures 3A–D. For $\tau \geq 10$ μs, the fit residuals were lower than 0.01. The residuals of cross-correlation data were lower than 0.005. These results show that satisfactory fits were obtained. In current study, the stable fluorescence fluctuations even with a relatively long detection time (120 s) showed negligible photobleaching. However, a build-up of triplet state in the current measurements were observed (typically 20% for red channel and 10% for green channel, and faint triplet states fraction in cross-correlation). With a Zeiss ConfoCor2 data reduction software, the auto- and cross-correlation functions were fitted to the eq 5. The physical parameters, such as diffusion time, particle numbers (N_g, N_r, N_{gr}), and the correlation values from a measurement, were corrected for the triplet states effects.

The system was tested with thrombin of various concentrations (0–20 nM). The results reveal a concentration dependent response. To achieve a more accurate calibration, the amplitude of cross-correlation function was normalized to that of auto-correlation function in the green channel, that is, $G_{gr}(0) - 1/G_g(0) - 1$. It was found that when the concentration of thrombin increased from 0 to 10 nM, the signal intensity increased correspondingly (see Figure 4). Thrombin concentration increased to that higher than 10 nM, the signal intensity decreased. This indicates that the equilibrium concentrations were achieved. When the cutoff line was defined as the mean plus 3 standard deviations of the control sample, the detection limit of 0.8 nM was achieved. Currently, both the Apt 15 and Apt 29 probe concentration are 2 nM. With a preliminary exploration, we found that when the probe concentrations were increased to 10 nM, the detectable dynamic range for thrombin could be extended to 30 nM, with a small sacrifice of the sensitivity (data not shown).

Three proteins, BSA, IgG, and AFP at concentration of 1 μM were used to test the specificity of this assay. The resulting signal was compared with that obtained using 10 nM thrombin, as shown in Figure 5. These experiments demonstrate a high specificity of the assay. High signal was obtained only when the

dx.doi.org/10.1021/ac1028648 |*Anal. Chem.* 2011, 83, 2906–2912

specific protein (thrombin) was tested, whereas the cross-correlation signals were negligible in the presence of BSA, IgG, and AFP.

A significant challenge for all protein analyses is the ability to be applied in a complex biological system. To demonstrate the feasibility of the assay in a complex biological system, thrombin spiked in serum was evaluated with the assay. Serum is that remains from whole blood after coagulation. Its chemical compositions are similar to that of plasma, but, not contain coagulation proteins such as thrombin or other factors. Serum, diluted 1:10, was tested alone or spiked with thrombin at three concentrations (1, 5, and 10 nM thrombin). Table 1 shows the resulted relative cross-correlation values, $G_{gr}(0) - 1/G_g(0) - 1$. The extraction recoveries of thrombin from the serum samples were measured based on the calibration graph using pure thrombin in buffer. The results show a 78% recoveries at 5 nM and 86% recoveries at 10 nM, respectively. Without detected signal was achieved when 1 nM thrombin was spiked in serum.

Table 1. Relative Cross-Correlation, $G_{gr}(0) - 1/G_g(0) - 1$, with 0, 1, 5, and 10 nM of Thrombin Detected in Buffer and in 10-Fold Diluted Serum

		in buffer			in diluted serum		
measurements (120s)	control	1 nM	5 nM	10 nM	1 nM	5 nM	10 nM
1	0.042	0.114	0.198	0.309	0.053	0.174	0.270
2	0.038	0.107	0.236	0.285	0.043	0.156	0.276
3	0.052	0.096	0.220	0.328	0.039	0.181	0.248
mean	0.044	0.106	0.218	0.307	0.045	0.170	0.265
s.d.	0.007	0.009	0.019	0.022	0.007	0.013	0.015

The reduced sensitivity in serum sample, compared to that in the buffer, may be attributed to certain serum components bind to or modify part of the protein and decrease its availability for binding to the aptamers. The s.d. values for detecting different concentrations of thrombin in buffer and diluted serum were ranged

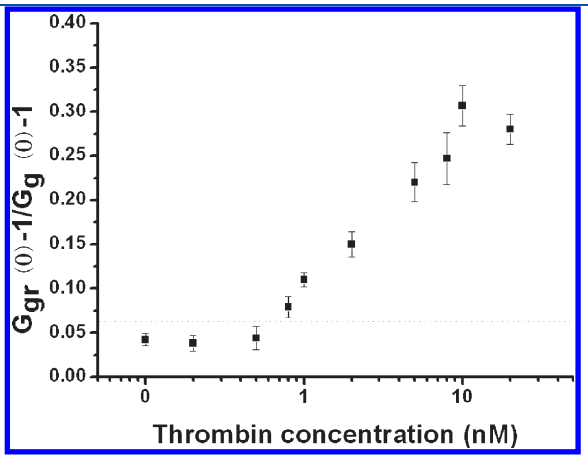

Figure 4. Relative cross-correlation, $G_{gr}(0) - 1/G_g(0) - 1$, with various concentrations of thrombin. For quantitative evaluation of cross-correlations, the amplitude of cross-correlation $[G_{gr}(0)]$ was normalized by that of autocorrelation $[G_g(0)]$. The concentration of this two aptamer probes is 2 nM, respectively. The measure time is 120 s. The standard deviations are derived from three independent measurements. The broken line indicates the cutoff value determined from the mean of control samples plus 3 standard deviations. Data are expressed as means ± standard deviations.

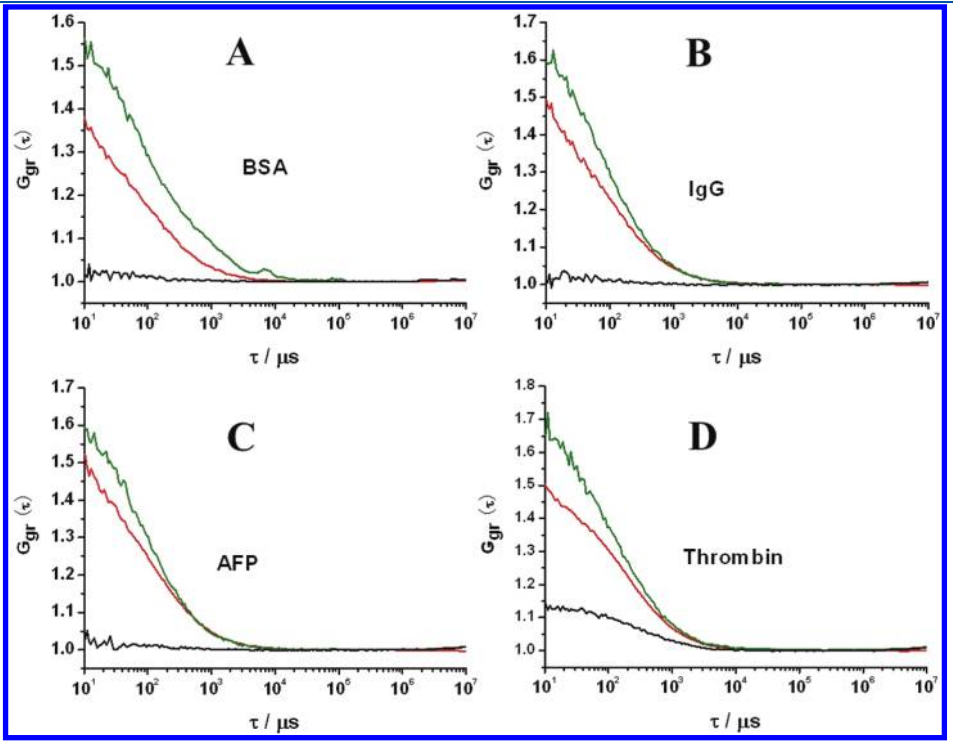

Figure 5. Evaluation of the specificity of current FCCS based thrombin detection method. Autocorrelation and cross-correlation signals from green labeled and red labeled aptamer probes in the presence of (A) 1 μM BSA; (B) 1 μM IgG; (C) 1 μM AFP; (D) 10 nM Thrombin. Red line indicates the autocorrelation curves from Cy5 labeled Apt29; green line indicates the autocorrelation curves from RG labeled Apt15; black line indicates the cross-correlation curves.

dx.doi.org/10.1021/ac1028648 |*Anal. Chem.* 2011, 83, 2906–2912

from 0.007 to 0.022. Such deviations in interval measurements should mainly be caused by variations in sample preparation.

DISCUSSION

By this study it is possible to use FCCS as a direct assay for protein detection. Compared with the established ELISA assay, current FCCS procedure stands outs for its advantages, such as (i) separation-free measurements, thus eliminating the washing steps used in ELISA to separate unbound from bound ligands; (ii) the minimal number of handling steps for sample preparation and the need of only microliters of sample.

Compared with other homogeneous assays, such as fluorescence polarization and FRET techniques, the main advantages can be summarized as following: (1) FCCS works well with large chromophore distances. For FRET, the efficiency of energy transfer between two fluorophores is used as a measure of molecular interaction. Therefore, application of FRET is sometimes limited because its efficiency is dependent on the relative orientation between the donor and acceptor fluorophores as well as the distance between them. Prior structural knowledge and control of linker flexibility is necessary to obtain appropriate placement of the chromophores. These requirements complicate experimental procedures and put limitations on the use of FRET for probing small molecules. FCCS can detect sandwich formation without such distance limitations. (2) Fluorescence polarization suffers from relatively poor specificity because of the noise arised from unspecific interactions between dye labeled aptamer probes and other unwanted species. (3) FRET-based techniques measure changes in light intensity, thus are susceptible to unpredictable quenching caused by environmental factors. In FCCS assay, probe-target complexes are identified by a simultaneous detection of two independent channels. In addition, FCCS also measures diffusion time rather than fluorescence signal alone, thus significantly improve the reliability of the assay. (4) Compared to FRET and fluorescence polarization that requires large sample volumes, the detection volume of FCCS was less than 1 fL. Because of the short transient time of individual fluorescent molecules and by optimizing the required optical parameters of the measurement device, photobleaching can be minimized. The femtoliter probe volume reduces the interference from background emission, thus the assay can be achieved at single molecule level.

In our measurements, the build-up of triplet states arise from blinking has been observed. Although quantitative analysis can be achieved by correcting these data, by increase the photostability of the probe, we may further enhance the reliability of the assay. As the build-up of triplet states reduces the total photon output and causes an underestimate of the actual analyte concentration. The may be achieved by further eliminating oxygen in the solution with a triplet quencher (such as Trolox) combined with others oxygen free-radicals scavengers.[46]

Even though the detection of protein with low-nanomolar sensitivity is achieved by this study, the sensitivity of the assay may be further improved with the probe quench method, as described in the literatures.[32,34,35] The sensitivity may also be improved by enhancing the quantum yield by bilabeling the probe[33] or by using a quantum dot label.[7]

Although in the current assay, two specific aptamers are used for FCCS measurement of a target protein, the method has the potential to be a general approach by spliting an aptamer into two subunits. This is because oligonucleotide aptamers generally consist of a single oligonucleotide chain comprised of two partially complementary domains. So in theory, most aptamers can be splited into two or more subunits. Some single strand aptamers, such as cocaine aptamer, hemin aptamer, HIV-1 aptamer, and thrombin aptamer, have been successfully splited.[47−50] Additional research with current general single molecule protein assay based on splited aptamer probes are being conducted in this lab.

Because aptamers can be easily created by in vitro selection for binding to a diverse range of targets with both high binding affinity and specificity, the presented single molecule assay may be applied to the detection of biological cofactors, metabolites, proteins, and a variety of other ligands of interest. We anticipate that the FCCS assay find numerous applications in this field. The present study provides the evidence as a proof-of-concept, thus opening a new direction for the development of one-step homogeneous protein detection with high sensitivity and excellent specificity.

ASSOCIATED CONTENT

Supporting Information. Figure showing the fluorescence intensities of RG-labeled Apt 15. This material is available free of charge via the Internet at http://pubs.acs.org.

AUTHOR INFORMATION

Corresponding Author

*Tel: (+86-20) 8521-0089. Fax: (+86-20) 8521-6052. E-mail: xingda@scnu.edu.cn.

ACKNOWLEDGMENT

This research is supported by the Key Program of NSFC-Guangdong Joint Funds of China (U0931005), the National Basic Research Program of China (2010CB732602; 2011CB910402), and the Program for Changjiang Scholars and Innovative Research Team in University (IRT0829).

REFERENCES

(1) Lequin, R. M. *Clin. Chem.* **2005**, *51*, 2415–2418.
(2) Engvall, E.; Perlmann, P. *Immunochemistry* **1971**, *8*, 871–874.
(3) Sun, B.; Xie, W.; Yi, G.; Chen, D.; Zhou, Y.; Cheng, J. *J. Immunol. Meth.* **2001**, *249*, 85–89.
(4) Tang, L.; Dong, C.; Ren, J. *Talanta* **2010**, *81*, 1560–1567.
(5) Stoevesandt, O.; Köhler, K.; Fischer, R.; Johnston, I. C.; Brock, R. *Nat. Meth.* **2005**, *2*, 833–835.
(6) Fujii, F.; Horiuchi, M.; Ueno, M.; Sakata, H.; Nagao, I.; Tamura, M.; Kinjo, M. *Anal. Biochem.* **2007**, *370*, 131–141.
(7) Fuji, F.; Kinjo, M. *ChemBioChem* **2007**, *8*, 2199–2203.
(8) Miller, A. E.; Hollars, C. W.; Lane, S. M.; Laurence, T. A. *Anal. Chem.* **2009**, *81*, 5614–5622.
(9) Ellington, A. D.; Szostak, J. W. *Nature* **1990**, *346*, 818–822.
(10) Tuerk, C.; Gold, L. *Science* **1990**, *249*, 505–510.
(11) Cho, E.; Lee, J.; Ellington, A. *Annu. Rev. Anal. Chem.* **2009**, *2*, 241–264.
(12) Xiang, Y.; Xie, M.; Bash, R.; Chen, J.; Wang, J. *Angew. Chem., Int. Ed.* **2007**, *46*, 9054–9056.
(13) Xue, L.; Zhou, X.; Xing, D. *Chem. Commun.* **2010**, *46*, 7373–7375.
(14) Xiao, Y.; Piorek, B. D.; Plaxco, K. W.; Heeger, A. J. *J. Am. Chem. Soc.* **2005**, *127*, 17990–17991.
(15) Liu, J.; Mazumdar, D.; Lu, Y. *Angew. Chem., Int. Ed.* **2006**, *45*, 7955–7959.

(16) Zhang, H.; Wang, Z.; Li, X.; Le, X. C. *Angew. Chem., Int. Ed.* **2006**, *45*, 1576–1580.
(17) Willner, I.; Zayats, M. *Angew. Chem., Int. Ed.* **2007**, *46*, 6408–6418.
(18) Jayasena, S. D. *Clin. Chem.* **1999**, *45*, 1628–1650.
(19) Li, J. J.; Fang, X.; Tan, W. *Biochem. Biophys. Res. Commun.* **2002**, *292*, 31–40.
(20) Hamaguchi, N.; Ellington, A. D.; Stanton, M. *Anal. Biochem.* **2001**, *294*, 126–131.
(21) Gokulrangan, G.; Unruh, J. R.; Holub, D. F.; Ingram, B.; Johnson, C. K.; Wilson., G. S. *Anal. Chem.* **2005**, *77*, 1963–1970.
(22) Fang, X.; Cao, Z.; Beck, T.; Tan, W. *Anal. Chem.* **2001**, *73*, 5752–5757.
(23) Yang, C. J.; Jockusch, S.; Vicens, M.; Turro, N.; Tan, W. *Proc. Natl. Acad. Sci. U.S.A.* **2005**, *102*, 17278–17283.
(24) Schwille, P.; Meyer-Almes, F. J.; Rigler, R. *Biophys. J.* **1997**, *72*, 1878–1886.
(25) Bacia, K.; Schwille, P. *Nat. Protoc.* **2007**, *2*, 2842–2856.
(26) Chen, Y.; Munteanu, A. C.; Huang, Y. F.; Phillips, J.; Zhu, Z.; Mavros, M.; Tan, W. *Chemistry* **2009**, *15*, 5327–5336.
(27) Widengren, J.; Dapprich, J.; Rigler, R. *Chem. Phys.* **1997**, *216*, 417–426.
(28) Dittrich, P. S.; Schwille, P. *Appl. Phys. B: Laser Opt.* **2001**, *73*, 829–837.
(29) Tcherniak, A.; Reznik, C.; Link, S.; Landes, C. F. *Anal. Chem.* **2009**, *81*, 746–754.
(30) Kettling, U.; Koltermann, A.; Schwille, P.; Eigen, M. *Proc. Natl. Acad. Sci. U.S.A.* **1998**, *95*, 1416–1420.
(31) Jahnz, M.; Schwille, P. *Nucleic Acids Res.* **2005**, *33*, e60.
(32) Nolan, R. L.; Cai, H.; Nolan, J. P.; Goodwin, P. M. *Anal. Chem.* **2003**, *75*, 6236.
(33) Korn, K.; Gardellin, P.; Liao, B.; Amacker, M.; Bergström, Å.; Björkman, H.; Camacho, A.; Dörhöfer, S.; Dörre, K.; Enström, J.; Ericson, T.; Favez, T.; Gösch, M.; Honegger, A.; Jaccoud, S.; Lapczyna, M.; Litborn, E.; Thyberg, P.; Winter, H.; Rigler, R. *Nucleic Acids Res.* **2003**, *31*, e89.
(34) Neely, L. A.; Patel, S.; Garver, J.; Gallo, M.; Hackett, M.; McLaughlin, S.; Nadel, M.; Harris, J.; Gullans, S.; Rooke, J. *Nat. Meth.* **2006**, *3*, 41–46.
(35) Földes-Papp, Z.; Kinjo, M.; Tamura, M.; Birch-Hirschfeld, E.; Demel, U.; Tilz, G. P. *Exp. Mol. Pathol.* **2005**, *78*, 177–189.
(36) Stoevesandt, O.; Köhler, K.; Fischer, R.; Johnston, I. C.; Brock, R. *Nat. Meth.* **2005**, *2*, 833–835.
(37) Földes-Papp, Z. *Exp. Mol. Pathol.* **2007**, *82*, 147–155.
(38) Stubbs, M. T.; Bode, W. *Thromb. Res.* **1993**, *69*, 1–58.
(39) White, R. R.; Sullenger, B. A.; Rusconi, C. P. *J. Clin. Invest.* **2000**, *106*, 929–934.
(40) Bock, L. C.; Griffin, L. C.; Lathan, J. A.; Vermaas, E. H.; Toole, J. J. *Nature* **1992**, *355*, 564–566.
(41) Tasset, D. M.; Kubik, M. F.; Steiner, W. *J. Mol. Biol.* **1997**, *272*, 688–698.
(42) Zhou, X.; Xing, D.; Tang, Y.; Chen, W. *PLoS one.* **2009**, *4*, e8074.
(43) Chen, X.; Zhou, Y.; Qu, P.; Zhao, X. S. *J. Am. Chem. Soc.* **2008**, *130*, 16947–16952.
(44) Neubauer, H.; Gaiko, N.; Berger, S.; Schaffer, J.; Eggeling, C.; Tuma, J.; Verdier, L.; Seidel, C. A.; Griesinger, C.; Volkmer, A. *J. Am. Chem. Soc.* **2007**, *129*, 12746–12755.
(45) Liang, L.; Wang, X.; Xing, D.; Chen, T. *J. Biomed. Opt.* **2009**, *14*, 024013.
(46) Taylor, J. N.; Darugar, Q.; Kourentzi, K.; Willson, R. C.; Landes, C. F. *Biochem. Biophys. Res. Commun.* **2008**, *373*, 213–218.
(47) Stojanovic, M. N.; Prada, P.; Landry, D. W. *J. Am. Chem. Soc.* **2000**, *122*, 11547–11548.
(48) Lu, N.; Shao, C.; Deng, Z. *Chem. Commun.* **2008**, 6161–6163.
(49) Yamamoto, R.; Kumar, P. K. R. *Gene Cells* **2000**, *5*, 389–396.
(50) Lin, Z.; Chen, L.; Zhu, X.; Qiu, B.; Chen, G. *Chem. Commun.* **2010**, *46*, 5563–5565.